

All-Ferrous Titanium(III) Citrate Reduced Fe Protein of Nitrogenase: An XAS Study of Electronic and Metrical Structure

Kristin B. Musgrave,[†] Hayley C. Angove,[‡]
Barbara K. Burgess,^{*,‡} Britt Hedman,^{*,§} and
Keith O. Hodgson^{*,†,§}

Department of Chemistry, Stanford University, and
Stanford Synchrotron Radiation Laboratory
Stanford, California 94305
Department of Molecular Biology and Biochemistry
University of California, Irvine, California 92697

Received February 23, 1998

Nitrogenase, which catalyzes the reduction of N_2 to NH_3 , is composed of two separately purified proteins, the MoFe protein and the Fe protein. The Fe protein contains a single Fe_4S_4 cluster bridged between two identical subunits. That cluster has long been believed to fluctuate between the 2+ and 1+ oxidation states during enzyme turnover.¹ This view was challenged in 1994, when evidence for the formation of an all-ferrous form of the Fe protein was obtained.² Recently Mössbauer and EPR experiments have confirmed the formation of an $[Fe_4S_4]^0$ state of the Fe protein following reduction by Ti(III) citrate, opening up the possibility that such a state could be physiologically relevant.³ As there are no model compounds with thiolate ligands in this oxidation state no structural information is available. Fe K-edge EXAFS analysis⁴ of the Ti(III) citrate reduced Fe protein provides the first metrical details of the unprecedented all-ferrous $[Fe_4S_4]^0$ cluster, whereas Fe–K and S–K edge studies provide information on electronic structural changes. EXAFS analysis was performed using the *ab initio* GNXAS data analysis method.^{5,6}

Three oxidation states of the Fe protein Fe_4S_4 cluster were analyzed: 2+ produced by indigo disulfonate (IDS) oxidation (1); 1+ produced by sodium dithionite (DT) reduction (2); and 0 produced by Ti(III) citrate reduction (3).⁷ The Fe–K X-ray absorption edge spectra (Figure 1) show the typical structure of an Fe_4S_4 cluster of approximately tetrahedrally coordinated Fe atoms with a prominent $1s \rightarrow 3d$ preedge transition at ~ 7112 eV and a relatively featureless rising edge with a shoulder at ~ 7119 eV.⁸ The edges gradually change with reduction. The rising edge exhibits a shift to lower energy of ~ 0.4 eV for the 1+ state (2) and ~ 0.9 eV for the 0 state (3) relative to the 2+ state (1). The intensity of the preedge transition is essentially the same for 1 and 2 but is reduced by $>50\%$ for 3, and there is also for the preedge transition a gradual shift to lower energy with reduction. There is also a progressive increase in intensity for the transition around 7126 eV with reduction, which is consistent with changes observed upon reduction for certain other Fe–S clusters.⁹

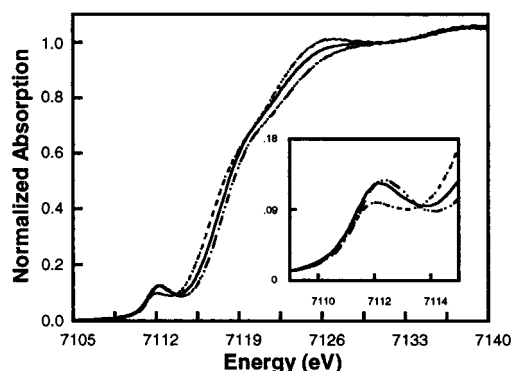


Figure 1. Normalized Fe K-edge spectra of the IDS oxidized (1) (- · · -), dithionite reduced (2) (—), and Ti(III) citrate reduced (3) (···) Fe protein samples. Inset: expansion of the $1s \rightarrow 3d$ preedge region showing the redox-dependent energy shift and intensity decrease.

The edge energy position reflects the effective nuclear charge at the photoabsorber. In general, the more reduced the oxidation state, the lower the edge energy. The progressive energy shift is thus a direct indication of the reduction at the iron atoms in the cluster. The $1s \rightarrow 3d$ transition is formally dipole forbidden but derives intensity mainly from electric-dipole $3d-4p$ mixing (which is high in a tetrahedral geometry).^{10–12} Several factors influence the $1s \rightarrow 3d$ energy position, intensity, and splitting into more than one transition, including the spin state and effective charge, geometry, and ligand type.¹² The observation that the $1s \rightarrow 3d$ transition is at lower energy and has a lower intensity for 3 is consistent with the Fe absorbers being at a lower formal oxidation state than those of 1 and 2.¹¹ Sulfur K-edge XAS data (Supporting Information) show that the first feature in the edge spectrum around 2470 eV (a $1s \rightarrow \psi^*$ transition¹³) is shifted toward higher energy by ca. 0.5 eV in 3. A lower effective nuclear metal charge leads to a higher binding energy for the d-orbitals which requires higher energy for this edge transition to appear.^{14,15} This observation thus again confirms that the 0 state of the cluster in 3 contains Fe atoms whose redox state is

(7) Purified *Azotobacter vinelandii* Fe protein (1850 nmol of H_2 /(min·mg)) was concentrated to >100 mg/mL using a Centricon 30 (Amicon). For all samples, DT was removed on a Sephadex G-25 column with Chelex treated 50 mM Tris-HCl pH 8.0, 5% glycerol, and 0.5 M NaCl. All samples were prepared in a Vacuum Atmospheres drybox under Ar. Fe–K XAS samples were filled in capped sample cells (plexiglass, 140 μ L, 37.5- μ m Kapton window) and frozen rapidly in liquid N_2 outside the box. S–K XAS samples were filled in a drybox (under N_2) in sealed anaerobic cells (6.25- μ m polypropylene window) and measured immediately. The 2+ sample was prepared using a column of IDS dye immobilized on an anion-exchange resin (Ashby, G. A.; Thornley, R. N. F. *Biochem. J.* **1987**, *246*, 445). The 1+ sample was prepared by exchanging into fresh buffer, 2 mM in DT. The 0 sample was prepared by addition of Ti(III) citrate; final concentration was 7–8 mM. Final Fe protein sample concentrations were between 0.95 and 1.9 mM. The oxidation states were confirmed by quantitative EPR analysis of a portion of the EXAFS samples frozen at the same time and of thawed EXAFS samples after the experiment. The 2+ and 0 oxidation states showed no $S = 3/2$ or $S = 1/2$ before or after the experiment. The 1+ sample exhibited some self-oxidation after thawing, which is not unexpected.¹ The activities of all samples were indistinguishable $\geq 80\%$ of initial activity (except for the 2+ state S–K edge sample at 60%) after thawing twice, once for EPR measurements, then for assaying, (three times for S–K edge samples).

(8) Arber, J. M.; Flood, A. C.; Garner, C. D.; Gormal, C. A.; Hasnain, S. S.; Smith, S. E. *Biochem. J.* **1988**, *252*, 421.

(9) Musgrave, K. B.; Liu, H. I.; Ma, L.; Burgess, B. K.; Watt, G.; Hedman, B.; Hodgson, K. O. *J. Biol. Inorg. Chem.* In press.

(10) Shulman, R. G.; Yafet, Y.; Eisenberger, P.; Blumberg, W. E. *Proc. Natl. Acad. Sci. U.S.A.* **1976**, *73*, 1384.

(11) Bair, R. A.; Goddard, W. A. *Phys. Rev.* **1980**, *B22*, 2767.

(12) Westre, T. E.; Kennepohl, P.; DeWitt, J. G.; Hedman, B.; Hodgson, K. O.; Solomon, E. I. *J. Am. Chem. Soc.* **1997**, *119*, 6297.

(13) Hedman, B.; Hodgson, K. O.; Solomon, E. I. *J. Am. Chem. Soc.* **1990**, *112*, 1643.

(14) Shadle, S. E.; Hedman, B.; Hodgson, K. O.; Solomon, E. I. *J. Am. Chem. Soc.* **1995**, *117*, 2259.

[†] Department of Chemistry, Stanford University.

[‡] University of California, Irvine.

[§] Stanford Synchrotron Radiation Laboratory, Stanford University.

(1) Burgess, B. K.; Lowe, D. J. *Chem. Rev.* **1996**, *96*, 2983.

(2) Watt, G. D.; Reddy, K. R. N. *J. Inorg. Biochem.* **1994**, *53*, 281.

(3) Angove, H. C.; Yoo, S. J.; Burgess, B. K.; Münck, E. *J. Am. Chem. Soc.* **1997**, *119*, 8730.

(4) Fe K-edge XAS spectra were obtained at Stanford Synchrotron Radiation Laboratory (SSRL): 8-pole wiggler station BL7-3; Si(220) double-crystal monochromator; detuned 50% at 8257 eV; fluorescence measurements using a 13-element Ge array detector; data represent average of 15, 14, and 15 scans for 1, 2, and 3; internal Fe foil calibration, first Fe foil edge inflection point assigned to 7111.2 eV. The S–K edge data were measured and analyzed as described in ref 15 with a sample temperature of $\sim +4$ °C.

(5) Filippini, A.; Di Cicco, A.; Natoli, C. R. *Phys. Rev. B* **1995**, *52*, 15122.

(6) Westre, T. E.; Di Cicco, A.; Filippini, A.; Natoli, C. R.; Hedman, B.; Solomon, E. I.; Hodgson, K. O. *J. Am. Chem. Soc.* **1995**, *117*, 1566.

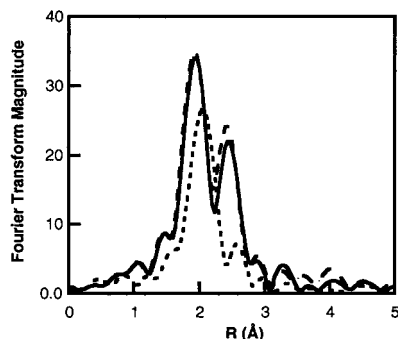


Figure 2. Comparison of non-phase shift corrected Fourier transforms of **1** (---), **2** (—), and **3** (···).

below that of **1** and **2** and, although as yet not quantified, indicates that S is not the major redox active component.

Dramatic differences are seen in the EXAFS Fourier transform of **3** as compared to **1** and **2** (Figure 2). In **3**, the first-shell peak has a decreased amplitude, has a somewhat broader FWHM, and is shifted to longer distance. The second-shell peak for **3** is likewise shifted to longer distance, and a reduction of ~65–75% in amplitude is seen. The decreased amplitude indicates a significantly less regular cluster structure, either a static disorder around an average distance, a distribution of discrete Fe–Fe distances, or a combination of both. Evidence that this does not result from a breakup of the cluster is provided by Mössbauer data³ and the fact that the redox process is reversible.² Excellent fits were obtained to the EXAFS data of **1** and **2** by assuming a typical Fe₄S₄ structure,¹⁶ and the results are consistent with previous studies of the 2⁺¹⁷ and 1⁺¹⁸ states. The σ^2 parameters (related to Debye–Waller factors; reflecting thermal vibration and static disorder) for both states were small and of the order expected for the symmetry and flexibility¹⁹ of these cluster types.

It was impossible to fit the data of **3** with an analogous Fe₄S₄ model of longer single Fe–S and Fe–Fe distances. The σ^2 parameters for the second shell consistently refined to very large values (>0.02 Å²) at a distance of 2.66 Å, and the EXAFS residual ($\chi^{\text{obs}} - \chi^{\text{fit}}$) clearly showed the presence of an unfit frequency. With the inclusion of a second Fe–Fe contribution at a short distance, this residual was completely eliminated, the overall quality of the fit was significantly improved (Table 1), and the second-shell Fourier transform peak was excellently fit. The best fit to the data was achieved by using a coordination number of 2 for a short Fe–Fe interaction at 2.53 Å and 1 for a long Fe–Fe interaction at 2.77 Å.²⁰ The interference of these two Fe–Fe waves accounts for the decreased amplitude of the second-shell peak in the Fourier transform (Figure 2). The Fe–Fe distance of 2.53 Å is intriguing, as it is much shorter than those seen in Fe₄S₄ model complexes of higher oxidation states (~2.75 Å).²¹ Similar short Fe–Fe distances were observed in the all-ferrous

(15) Rose Williams, K.; Hedman, B.; Hodgson, K. O.; Solomon, E. I. *Inorg. Chim. Acta* **1997**, *263*, 315.

(16) 2⁺: 4S @ 2.27 Å, σ^2 0.002 Å², 3Fe @ 2.72 Å, σ^2 0.004 Å². 1⁺: 4S @ 2.29 Å, σ^2 0.002 Å², 3Fe @ 2.73 Å, σ^2 0.005 Å². *k*-range 4.2–15 Å⁻¹; *k*²-weighted.

(17) Ryle, M. J.; Lanzilotta, W. N.; Seefeldt, L. C.; Scarrow, R. C.; Jensen, G. M. *J. Biol. Chem.* **1996**, *271*, 1551.

(18) Lindahl, P. A.; Teo, B.-K.; Orme-Johnson, W. H. *Inorg. Chem.* **1987**, *26*, 3912.

(19) Berg, J. M.; Holm, R. H. In *Iron–Sulfur Proteins*; Spiro, T. G., Ed.; Wiley-Interscience: New York, 1982, Chapter 1.

(20) The numbers of short and long Fe–Fe distances were systematically varied keeping the sum fixed to 3. The distances remained within 0.03 and 0.01 Å, respectively, of the values in Table 1 throughout. The best fit with a 1:2 (short:long) distribution had a 14% relative increase in fit function value and with the σ^2 values strongly reversed in relative magnitude (0.002 and 0.008 Å², respectively).

Table 1. GNXAS Fit Results for the [Fe₄–S₄]⁰ State^a

Fe–S (Å)	2.35	2.37	2.29
coord no.	4	4	1
σ^2 (Å ²)	0.002	0.005	0.002
Fe–S (Å)			2.39
coord no.			3
σ^2 (Å ²)			0.003
Fe–Fe (Å)	2.66	2.53	2.52
coord no.	3	2	2
σ^2 (Å ²)	0.024	0.007	0.008
Fe–Fe (Å)		2.77	2.77
coord no.		1	1
σ^2 (Å ²)		0.005	0.005
$R(\text{fit})$	0.278×10^{-6}	0.162×10^{-6}	0.159×10^{-6}

^a *k*³-weighted data fit in the *k*-range 4.2–17 Å⁻¹

P^N state of the nitrogenase P clusters.^{9,22} A single Fe–S wave with a coordination number of 4 at a distance of 2.36 Å was also established, consistent with the higher R of the first-shell peak in the Fourier transform. This Fe–S distance is significantly longer than those in the lower oxidation state clusters.²³

Although the Fe–S σ^2 value was low, fits were also performed using two Fe–S contributions and, as shown in Table 1, the inclusion of a second Fe–S wave made a minor improvement to the quality of the fit.²⁴ The best split-shell fit to the data was achieved with 1 short Fe–S distance of 2.29 Å and 3 long Fe–S distances at 2.39 Å. A possible structural model with a 1:3 short-to-long Fe–S distribution and a 2:1 short-to-long Fe–Fe distribution is that of a compressed Fe₄S₄ cluster, in which the “vertical” Fe–Fe and Fe–S distances are shorter and the “horizontal” Fe–Fe and Fe–S distances and the Fe–S(thiolate) distances are longer.²⁵ Such a model would be consistent with the increased trend in flexibility established for models in the 2⁺ vs the 1⁺ state²⁶ and would give an expansion of the volume of the Fe₄S₄ cube from 11.85 Å³ (2⁺) to 12.17 Å³ (1⁺) to 13.14 Å³ (0) upon reduction. This work thus provides the first metrical details of an all-ferrous [Fe₄S₄]⁰ cluster.

Acknowledgment. This research has been supported by grants from NSF CHE-9423181 and NIH RR-01209 (K.O.H.) and NIH GM-43144 (B.K.B.). SSRL operations are funded by the DOE, Office of Basic Energy Sciences. The Biotechnology Program is supported by the NIH, National Center for Research Resources, Biomedical Technology Program, and by the DOE, Office of Biological and Environmental Research.

Supporting Information Available: S K-edge spectra, EXAFS data and final fits, and Fourier transforms of data and final fits for **1–3** (11 pages, print/PDF). See any current masthead page for ordering information and Web access instructions.

JA980598Z

(21) Carney, M. J.; Papaefthymiou, G. C.; Spertalian, K.; Frankel, R. B.; Holm, R. H. *J. Am. Chem. Soc.* **1988**, *110*, 6084.

(22) Peters, J. W.; Stowell, M. H. B.; Soltis, S. M.; Finnegan, M. G.; Johnson, M. K.; Rees, D. C. *Biochemistry* **1997**, *36*, 1181.

(23) Error analysis performed as described in the following: Zhang, H. H.; Filipponi, A.; Di Cicco, A.; Lee, S. C.; Scott, M. J.; Holm, R. H.; Hedman, B.; Hodgson, K. O. *Inorg. Chem.* **1996**, *35*, 4819 and references therein. Contour plots of all Fe–S/Fe–Fe distance combinations for both sets of fits showed, at 95% confidence level, maximum errors of ±0.02 Å for both Fe–Fe distances and ±0.01 Å for all Fe–S distances. The highest correlation was between the 2.53 Å Fe–Fe and 2.39 Å Fe–S distances (2 Fe–S wave fit) or the two Fe–Fe distances (1 Fe–S wave fit).

(24) The significance of the improvement is questionable. The fit function value and the σ^2 values decrease when two Fe–S interactions are included. The higher σ^2 values in the fits which included only one Fe–S interaction may also be the result of a range of Fe–S distances. The total coordination number for the Fe–S interactions was fixed to 4, while the contributions from the two distances were systematically varied by increments of 1.

(25) While the improvement seen when a second Fe–S interaction is included was small and does not definitively prove the existence of two Fe–S distances, a cluster model with this distribution is easier to construct.

(26) Beinert, H.; Holm, R. H.; Münck, E. *Science* **1997**, *277*, 653.